C. R. Geoscience 349 (2017) 53–62

Contents lists available at ScienceDirect

Comptes Rendus Geoscience

www.sciencedirect.com

Petrology, Geochemistry

Zircon U–Pb ages and Sr–Nd isotope ratios for the Sirstan granitoid body, NE Iraq: Evidence of magmatic activity in the Middle Cretaceous Period

Imad Kadhim Abdulzahra [a,d,*], Ayten Hadi [a], Hossein Azizi [b], Yoshihiro Asahara [c], Koshi Yamamoto [c]

[a] Department of Earth Science, College of Science, University of Baghdad, Baghdad, Iraq
[b] Mining Department, Faculty of Engineering, University of Kurdistan, Sanandaj, Iran
[c] Department of Earth and Environmental Sciences, Graduate School of Environmental Studies, Nagoya University, Nagoya, 464-8601, Japan
[d] Iraq Geological Survey, Al-Andalus Square, Baghdad, Iraq

ARTICLE INFO

Article history:
Received 6 August 2016
Accepted after revision 28 February 2017
Available online 24 April 2017

Handled by Marc Chaussidon

Keywords:
Sirstan
Middle Cretaceous
Sanadaj–Sirjan Zone
Zircon U–Pb age
I-type granite

ABSTRACT

The Sirstan granitoid (SG), comprising diorite and granodiorite, is located in the Shalair Valley area, in the northeastern part of Iraq within the Sanandaj–Sirjan Zone (SSZ) of the Zagros Orogenic Belt. The U–Pb zircon dating of the SG rocks has revealed a concordia age of 110 Ma, which is interpreted as the age of crystallization of this granitoid body during the Middle Cretaceous. The whole-rock Rb–Sr isochron data shows an age of 52.4 ± 9.4 Ma (*MSWD* = 1.7), which implies the reactivation of the granitoid body in the Early Eocene due to the collision between the Arabian and Iranian plates. These rocks show metaluminous affinity with low values of Nb, Ta and Ti compared to chondrite, suggesting the generation of these rocks over the subduction zone in an active continental margin regime. The SG rocks are hornblende-bearing I-type granitoids with microgranular mafic enclaves. The positive values of ε_{Nd} (t = 110 Ma) (+0.1 to +2.7) and the low $(^{87}Sr/^{86}Sr)_i$ ratios (0.7044 to 0.7057) indicate that the magma source of the SG granitoids is a depleted subcontinental mantle. The chemical and isotope compositions show that the SG body originated from the metasomatic mantle without a major role for continental contamination. Our findings show that the granitoid bodies distributed in the SSZ were derived from the continuous Neo-Tethys subduction beneath the SSZ in Mesozoic times and that the SSZ was an active margin in the Middle Cretaceous.

1. Introduction

The Sanandaj–Sirjan Zone (SSZ) is a part of the Zagros Orogenic Belt (ZOB), which is a member of the Alpine–Himalayan Orogenic Belt. The Zagros Belt comprises several NW–SE-trending zones that were formed as a consequence of the opening and closure of the Neo-Tethys Ocean beneath the Iranian Plate (Agard et al., 2005; Alavi, 1980, 1994; Berberian and Berberian, 1981; Berberian and King, 1981; Sengor, 1990). The ZOB of Iran consists of three parallel tectonic subdivisions trending NW to SE (Alavi, 1994):

- the Zagros Simply Folded Belt;
- the Sanandaj–Sirjan Zone (SSZ);
- the Urumieh–Dokhtar Magmatic assemblage (UDMA) (Fig. SM 1).

* Corresponding author: Department of Earth Science, College of Science, University of Baghdad, Iraq.
E-mail address: emadalsaffi@yahoo.com (I.K. Abdulzahra).

http://dx.doi.org/10.1016/j.crte.2017.02.004
1631-0713/

The reported ages for the granitoid plutons in the SSZ range from Neoproterozoic (Hassanzadeh et al., 2008) to Tertiary (Mahmoudi et al., 2011; Sepahi et al., 2014). The Paleozoic granitoid rocks are less distributed in the Iranian Plate and are related to the extensional intracontinental regime that accompanied the rifting of the Arabian Plate and the opening of the Neo-Tethys (e.g., Abdulzahra et al., 2016; Alirezaei and Hassanzadeh, 2012; Bea et al., 2011; Shafaii Mogadam et al., 2015; Shakerardakani et al., 2015). The majority of the granitoid rocks belong to the Middle to Late Jurassic and are linked to the subduction of the Neo-Tethys Ocean beneath the Iranian Plate (e.g., Ahmadi Khalaji et al., 2007; Azizi et al., 2011, 2015; Chiu et al., 2013; Esna-Ashari et al., 2012; Fazlnia et al., 2009; Hassanzadeh and Wernicke, 2016; Mahmoudi et al., 2011; Omrani et al., 2008; Shahbazi et al., 2010). However, little is known about the Cretaceous granitoid rocks in the SSZ as compared with the Jurassic granitoids. Zircon U–Pb age of the Hasan Salary I-type granites is 108.8 ± 0.3 Ma (Mahmoudi et al., 2011) and linked to the subduction-related magmatism of the Neo-Tethys Ocean beneath the Iranian Plate. Mazhari et al. (2011) dated the Naqadeh complex and reported a crystallization age of 96 ± 2.3 Ma. Cretaceous K–Ar and Rb–Sr ages were reported in the SSZ (e.g., Baharifar et al., 2004; Masoudi et al., 2002). These K–Ar and Rb–Sr isotope data show resetting of variable degrees by secondary processes (Mahmoudi et al., 2011) and are useful to estimate the tectonic and metamorphic events (Allègre, 2008; Asmerom et al., 1991; Evans, 1995) that occurred in the SSZ rather than those of crystallization.

In this study, a new radiometric age as well as chemical and Sr–Nd isotopic data are reported from the Sirstan granitoid rocks (SG) in the Shalair Valley within the SSZ in northeastern Iraq (the details of the analytical techniques are supplied as supplementary material). The present study throws light on the existence of a Cretaceous igneous activity that was previously considered to be a magmatic gap in the SSZ, as reported by Chiu et al. (2013).

2. Geological setting and sampling

The Sirstan granitoid body is located in the Shalair Valley area within the so-called Iraqi Suture Zone in northeastern Iraq near the Iraqi–Iranian border. This zone is considered as part of the Zagros Orogenic Belt (ZOB) that extends ca. 2000 km from Southeast Turkey through northeastern Iraq–northwestern Iran to northern Oman (Fig. SM 1; Alavi, 1994). This zone is linked to the Neo-Tethys Ocean and thrusted over the Arabian Plate in the Late Cretaceous obduction followed by collision during Miocene–Pliocene times (Jassim and Goff, 2006). The Zagros Suture Zone in northeastern Iraq is divided into three units that trend parallel to the main trend of the Zagros Belt, including the Qulqula–Khwakurk, Penjween–Walash and Shalair units (Buday and Jassim, 1987; Jassim and Goff, 2006) (Fig. 1a). The Shalair unit is located within the Shalair Valley area and is considered as part of the Sanandaj–Sirjan Zone. Structurally, the Shalair Valley is an eroded east–west-trending asymmetrical anticline whose axis gently plunges toward the east (Smirnov and Nelidov, 1962). It extends approximately over 30 km with a width of more than 20 km. The value of the dip ranges from 30° to 70° for the southern limb and from 20° to 40° for the northern limb (Smirnov and Nelidov, 1962). The core of the Shalair anticline is composed of metasedimentary sequences (Qandile Rock Series), whereas the limbs comprise the Katar Rash Volcanic Unit (also known as the Walash "Volcanic" Rock Series; Al-Shible and Kettaneh, 1972; Smirnov and Nelidov, 1962; Fig. 1b) that ranges in composition from basic to acidic igneous rocks (Al-Shible and Kettaneh, 1972; Buday and Jassim, 1987; Jassim and Goff, 2006). The Qandile Rock Series covered the majority of the Shalair Valley area and comprise 2000 m (Smirnov and Nelidov, 1962) of phyllite, schist, slate and greywacke with minor felsic volcanic and some lenticular limestone (Buday and Jassim, 1987; Jassim and Goff, 2006; Smirnov and Nelidov, 1962). The contact with the overlying Katar Rash Series is unclear, maybe gradational contact or low-angle unconformity (Jassim and Goff, 2006). Based on microfacies analyses, the estimated age of the Qandile Rock Series is Aptian–Cenomanian. However, a geochronological study is required to confirm this age. The Qandile Rock Series are reported to be formed in a fore-arc basin in front of the subduction zone (Jassim and Goff, 2006). The Katar Rash Series (also known as the Walash "Volcanic" Rock Series; Al-Shible and Kettaneh, 1972; Smirnov and Nelidov, 1962) are exposed along the limbs of the Shalair anticline and comprise 1000 m of calc-alkaline series of basaltic andesite, andesite, dacite and rhyolite (Jassim and Goff, 2006). This unit has been dated using U–Pb zircon age and yielded a crystallization age of ca. 108 ± 2.9 Ma (Ali et al., 2016).

Several granitoid bodies with variable dimensions crop out within the Shalair anticline; these are: Aulan, Sirstan, Laladar and Mishao which are exposed at the limbs within the Katar Rash Volcanic Unit and one body, the Damamna is exposed in the core within Qandile Rock Series (Abdulzahra et al., 2016; Al-Hafdh and Qasim, 1992; Al-Rubaie, 1976; Al-Shible and Kettaneh, 1972; De Villiers, 1957; Smirnov and Nelidov, 1962).

Various ages have been reported concerning the igneous activities in the Shalair Valley. Al-Shible and Kettaneh (1972) and Smirnov and Nelidov (1962) suggested that the igneous activity was during the Tertiary. Buday and Jassim (1987) and Jassim and Goff (2006) estimated that the Shalair Valley igneous activity was in the Late Cretaceous. Al-Hafdh and Qasim (1992) proposed Late Cretaceous to late Miocene. However, these estimated ages are based on field observation and correlation with the Upper Cretaceous igneous activities in the SSZ. For more details on the geology of the Shalair Valley area (see Jassim and Goff, 2006).

Cretaceous magmatic activities are well developed in the northwestern part of the SSZ compared with the southeastern part (Azizi and Moinevaziri, 2009; Mohajjel et al., 2003). In the northwestern part of the SSZ, the country rocks are composed mainly of shale, sandstone and calcareous rocks, which are intercalated, by basalt, andesitic basalt and andesite. These rocks show calc-alkaline magmatic affinity and are linked with a continental arc setting during the subduction of the Neo-Tethys Ocean beneath SSZ (Azizi and Jahanjiri, 2008; Azizi and

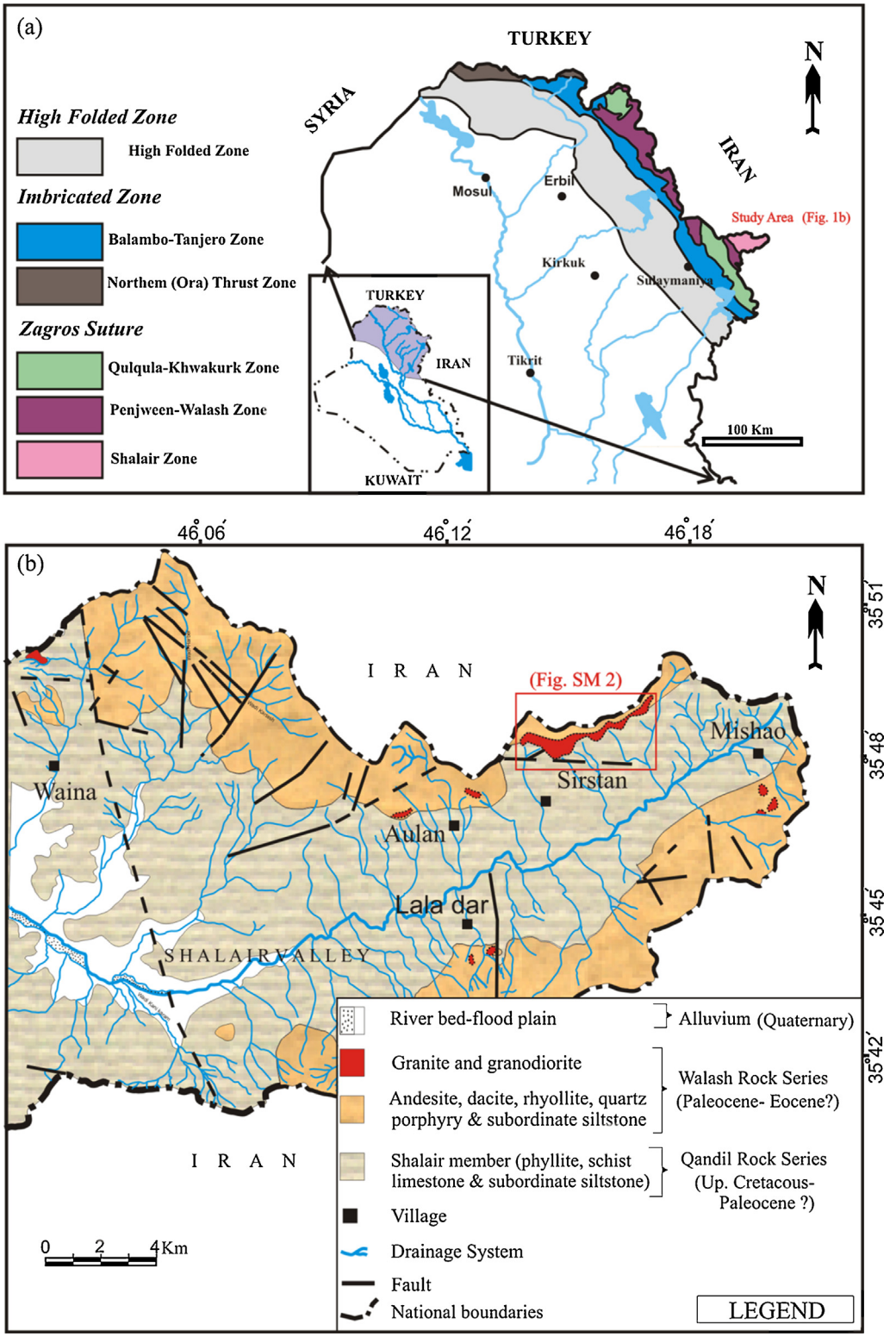

Fig. 1. a: tectonic zones of the Iraqi Zagros Suture Zone (Jassim and Goff, 2006), showing the distribution of igneous and metamorphic rocks; b: geological map of the Shalair Valley area from Al-Shible and Kettaneh (1972), modified.

Moinevaziri, 2009). Azizi and Moinevaziri (2009) suggested that the metasomatized mantle was responsible for introducing calc-alkaline magmatism during the subduction of Neo-Tethys Ocean. These magmatic activities were developed to form the magmatic arc system in the northwestern part of the SSZ.

In this study, we focus on the Sirstan granitoid (SG). The present new geochemical and geochronological data on the Sirstan rocks add new information on events in continuation with the events that occurred in the Sanandaj–Sirjan Zone and cover the missing age (Middle Cretaceous). Therefore, we employed the geochemical data and age relationship of the Siristan rocks, which seem to be important in the study of magmatic and tectonic history in Zagros Belt. The SG body is located to the north of the Sirstan village close to the Iranian border (Fig. SM 2). It is the largest intrusive body in the Valley and extends for about 5 km. This body is characterized by a very steep slope with rugged topography and is surrounded by volcanic rocks of Katar Rash from the north and phyllite rocks of Qandil Rock Series from the south (Fig. SM 2, SM3a). The contact relation between the SG and the surrounding rocks is not so clear (Al-Shible and Kettaneh, 1972; De Villiers, 1957; Smirnov and Nelidov, 1962). Generally, the rocks are gray to greenish gray in color, massive, coarse grained, fractured (Fig. SM 3a, b) and are cut by numerous quartz and epidote veins. Numerous mafic enclaves were noted within the coarse granitoid rocks throughout the Sirstan granitoid body. These enclaves show variable shapes and some are spherical, elliptical with sharp contact with the hosted granitoids. Their lengths are from a few centimeters to more than 15 cm; they are apparently finer grained than the surrounding or enclosing rocks (Fig. SM 3c, d).

3. Results

3.1. Petrography

The rock samples of the Sirstan pluton are composed mainly of plagioclase (45%), quartz (38%) and hornblende with minor amount of pyroxene (9%). Zircon, sphene and magnetite are the accessory minerals identified making approximately 7%, with sericite, epidote and chlorite as alteration products. The SG samples show an equigranular texture. According to the extinction angle measurement, the average plagioclase composition is from albite to oligoclase. They are subhedral and show variable size (0.3–3.0 mm) with an average of approximately 1.4 mm. Some of the plagioclase grains display deformation twins and fracturing (Fig. 2a). The quartz grains are anhedral with an average size of approximately 1.2 mm and a few of them show undulose extinction (Fig. 2b). The mafic minerals are dominated by hornblende, with minor pyroxene (augite), which are observed in all the studied samples, and make about 5 to 25 percent by volume. The grains are generally fresh and have well developed cleavage (Fig. 2c). They are subhedral to anhedral, greenish brown to faint brown in color and are peleocroic. In some thin sections, hornblende contains inclusions of plagioclase, quartz and opaque minerals (Fig. 2d, e). Some grains are altered due to an urilitization process along the grain boundaries and cracks. Opaque minerals are mostly magnetite, which occurs as single euhedral grains or as disseminated very fine-grained aggregates associated with highly deformed and altered regions. The enclave samples exhibit more or less similar mineralogical and textural features to the enclosing host granitoids, but are finer grained than the host and constitute more mafic minerals that are mainly hornblende along with minor amounts of biotite. These mafic minerals are surrounded by quartz and plagioclase forming a microgranular texture (Fig. 2f).

3.2. Whole-rock geochemistry

The analytical results of the major oxides in weight percent and the trace elements including REEs in ppm are listed in Table SM 1. The Sirstan granitoid and the enclave sample have moderate contents of SiO_2 (57.0–61.4 wt.%), high Al_2O_3 (15.3–16.7 wt.%) and ($Na_2O + K_2O$) (3.85–5.47 wt%). These rocks contain 0.62–0.74 wt.% TiO_2, 6.6–8.8 wt.% Fe_2O_3, 2.5–4.0 wt.% MgO and 2.7–7.1 wt.% CaO contents. The enclave sample (XeS) shows relatively less CaO, and high Fe_2O_3 and Na_2O contents than the enclosing host SG granitoids.

The SG rock samples show a good fractionation trend of major and trace elements with SiO_2 when plotted on the variation diagrams (Fig. SM 4).

In the alkali versus silica diagram (Middlemost, 1985), all samples of the SG and the enclave sample (XeS) are plotted in the diorite field with few SG samples along the border between diorite and granodiorite fields (Fig. SM 5a) and are calc-alkaline on the AFM diagram (Fig. SM 5b: Irvine and Baragar, 1971). On $Al_2O_3/(CaO + Na_2O + K_2O)$ versus $Al_2O_3/(Na_2O + K_2O)$ of Shand (1943) (Fig. SM 5c), the SG samples are defined as metaluminous with ASI values less than one, whereas the enclave sample has peraluminous affinity.

The chondrite-normalized REE patterns (normalization after Sun and McDonough, 1989) for the SG rocks are homogeneous (Fig. 3a) with fractionation REE (10 to 40 times chondrite) and slight LREE enrichment $(La/Yb)_N = 1.9–2.5$ (Table SM 1). The patterns show negative Eu anomalies ($Eu/Eu^* = 0.83–0.97$) that indicate plagioclase fractionation during the melting and crystallization stages. The REE pattern for the enclave sample more or less runs parallel to the host rock patterns, but shows relative enrichment with respect to the host granitoids with lower $(La/Yb)_N$ (= 1.3) and more pronounced negative Eu anomaly ($Eu/Eu^* = 0.54$). On the primitive mantle–normalized multi-component element diagram (normalization after Sun and McDonough, 1989) (Fig. 3b), the SG samples show a good consistency in the distribution of the elements with high amounts of K, Rb, and Pb, which are probably due to alteration, and distinct Nb, Ta and Ti depletions, which are characteristic geochemical indicators of subduction-related calc-alkaline magma (Pearce et al., 1984). The enclave sample exhibits a geochemical similarity with the host rocks, but is more depleted in Nb, Ta, and Ti, and slightly more enriched in HREE.

On the 10,000 × Ga/Al-versus-Nb diagram (Fig. SM 6a), the SG samples and enclave samples are plotted in the

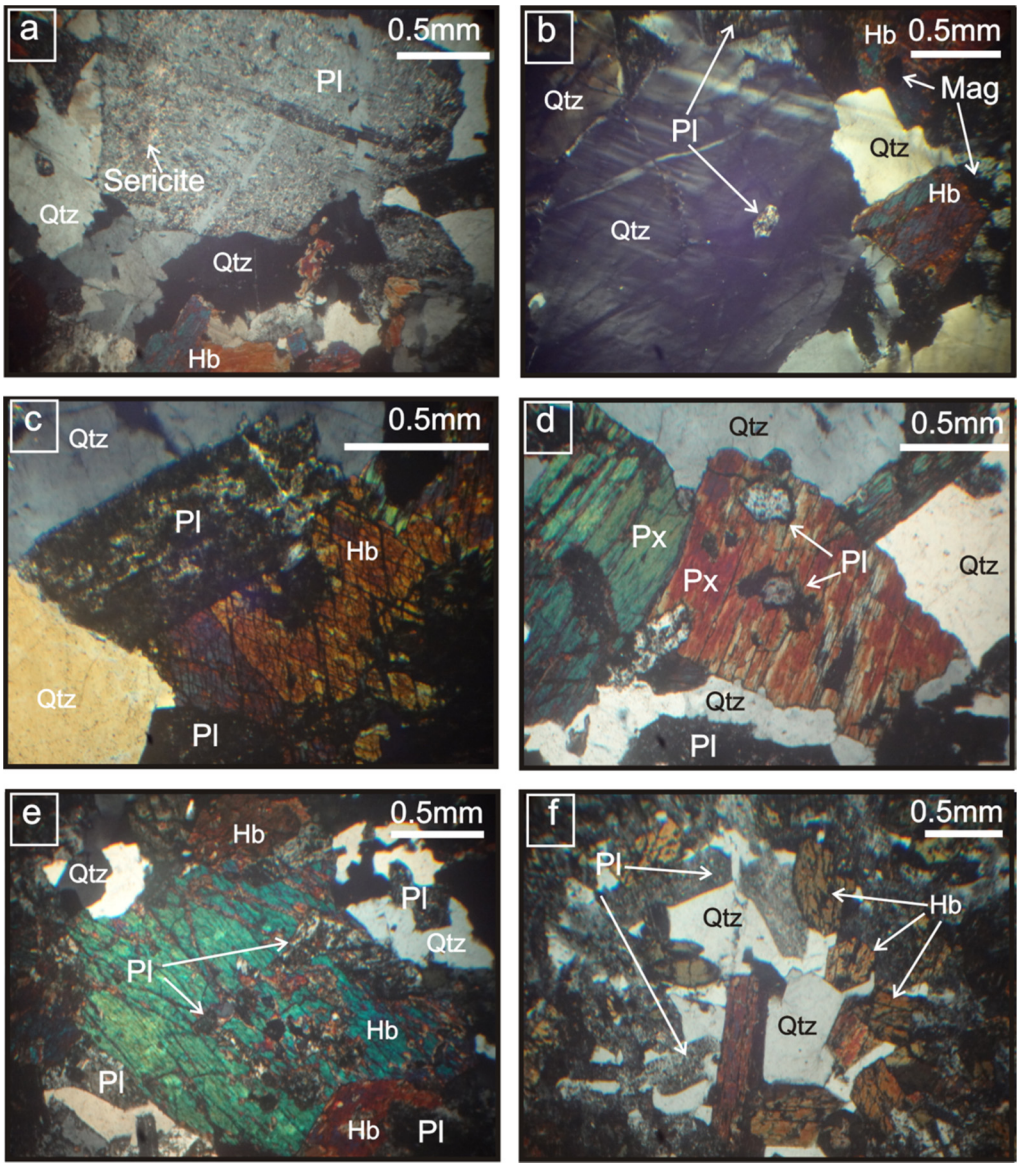

Fig. 2. Photomicrographs of the SG. a: deformation twins lamellae in plagioclase; b: undulose extinction in quartz; c: fresh hornblende with altered plagioclase; d, e: plagioclase imbedded in pyroxene; f: mineralogy of enclave samples, showing similar mineral composition with the host SG rocks. Symbols: Pl = plagiocalase; Qtz = quartz; Mag = magnetite; Hb = hornblende and Px = pyroxene.

M-S-I-type fields. The average values of 10,000 × Ga/Al ratios for the studied rocks of the SG and enclave (Table SM 1) are similar to the average values of I-type granitoids proposed by Whalen et al. (1987).

3.3. U–Pb zircon geochronology

Two samples (SG1 and SG2) were selected for zircon U–Pb age determination. The zircon grains are elongated, with lengths up to 250 μm. CL images (Fig. SM 7a, b) show that some zircon grains have zoning. And the zircon grains have microfractures that have affected grain size and shape. This could be due to deformation processes or to crushing of the rock sample during preparation.

The U–Pb analytical results of the selected zircon grains are listed in Table SM 2. According to the estimates from ^{204}Pb intensity measured by LA–ICP–MS analysis, these zircon grains have low common lead contents (about 2% for SG1 and SG2).

The values of the Th/U ratio of the zircon grains for SG1 and SG2 are 0.75 and 0.59, respectively, from which a magmatic origin can be inferred (Chen et al., 2007; Hartmann and Santos, 2004; Hoskin and Schaltegger, 2003; Rubatto, 2002). Both rims and cores for the zircon grains have the same age (Table SM 2). The U–Pb ages of the SG samples are calculated using ISOPLOT v. 4.15 software (Ludwig, 2012) and are 109.3 ± 1.3 Ma, with a mean square weighted deviate (MSWD) value of 1.4 for sample SG1

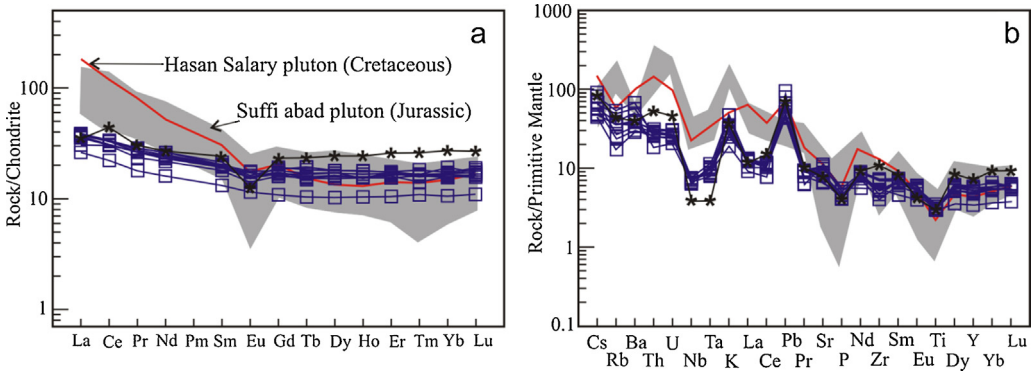

Fig. 3. a and b: REE patterns in the SG samples normalized by chondrite and primitive mantle, respectively (normalization after Sun and McDonough, 1989). See text for details. Data for the Suffi abad pluton from Azizi et al. (2011) and the Hasan Salary pluton from Mahmoudi et al. (2011) are shown for comparison. The star symbol indicates an enclave sample.

and 114.9 ± 4.9 Ma (*MSWD* = 9.5) for sample SG2 (Fig. 4a, b). Because of approximately similar results of the two-concordia ages, a weighted average age of 109.7 ± 1.3 Ma is taken as the crystallization age of the SG, which is in correspondence with the Middle Cretaceous period (i.e. Albian).

3.4. Rb–Sr whole-rock isochron

Eight out of nine samples were used to calculate Rb–Sr isochron. The excluded sample (S17) is slightly altered and it falls slightly off the isochron. The whole-rock Rb–Sr isochron system for the SG rocks shows a regular linear distribution of points (Fig. 5) and gives an age of 52.4 ± 9.4 Ma with a *MSWD* of 1.7, which is younger than the zircon U–Pb age (110 Ma). This is probably attributed to an incomplete reset of the whole-rock Rb–Sr isotope system during alteration and/or metamorphism processes (Allègre, 2008; Asmerom et al., 1991; Evans, 1995). This Rb–Sr data can be used to discuss the tectonic and metamorphic events that occurred in the area within Northeast Iraq and Northwest Iran during Paleogene period (i.e. the Eocene). It is possibly related to evidence of final closure of the Neo-Tethys (Ghasemi and Talbot, 2006; Jassim and Goff, 2006; Kazmin, 1991; Mazhari et al., 2009; Sharland et al., 2001; Vergès et al., 2011).

3.5. Sr and Nd isotope ratios

The results of our isotope analyses for Rb–Sr and Sm-Nd are listed in Table SM 3.

The initial values of both Sr and Nd isotope ratios ($^{87}Sr/^{86}Sr$, $^{143}Nd/^{144}Nd$) for the SG and the enclave rocks were calculated based on the U–Pb zircon age of 110 Ma. The values of $^{143}Nd/^{144}Nd$ (i) vary between 0.51250 and 0.51263, with positive ε_{Nd} (110 Ma) values ranging from +0.1 to +2.7, indicating mantle origin for both SG and enclave rocks. The initial $^{87}Sr/^{86}Sr$ values range from 0.7044 to 0.7057 for SG rocks which is the characteristics of I-type granites (Chappell and White, 1974, 1992). Armstrong et al. (1977) and Chappell and White (1974) suggested a critical boundary of 0.7060 for $^{87}Sr/^{86}Sr$ value with I-type granites having initial $^{87}Sr/^{86}Sr$ ratios between 0.7040 and 0.7060. Pitcher (1979) suggested

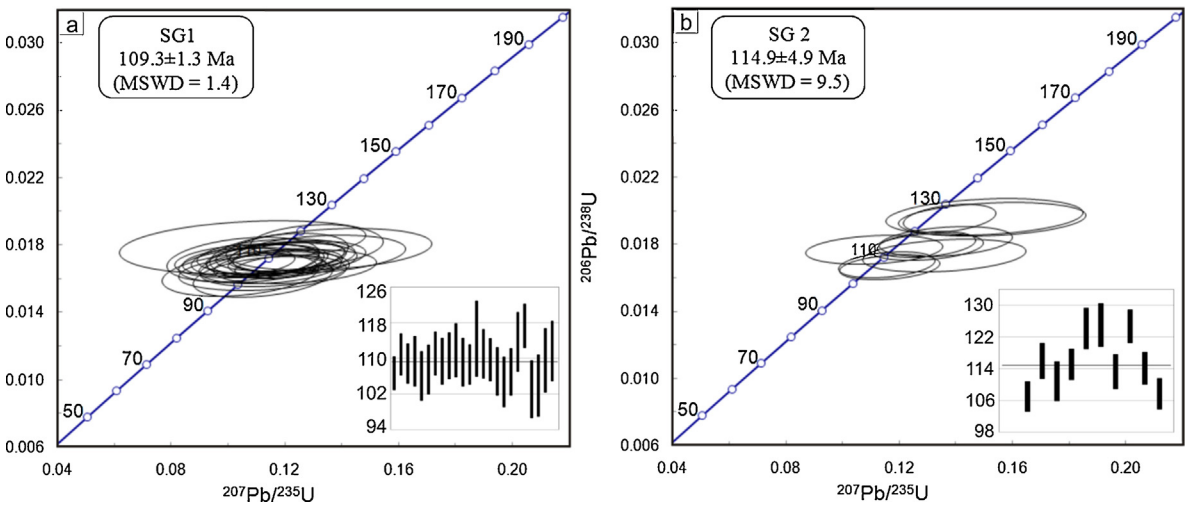

Fig. 4. U–Pb concordia ages for the SG. a: SG1 and b: SG2. Data-point error ellipses are 2σ.

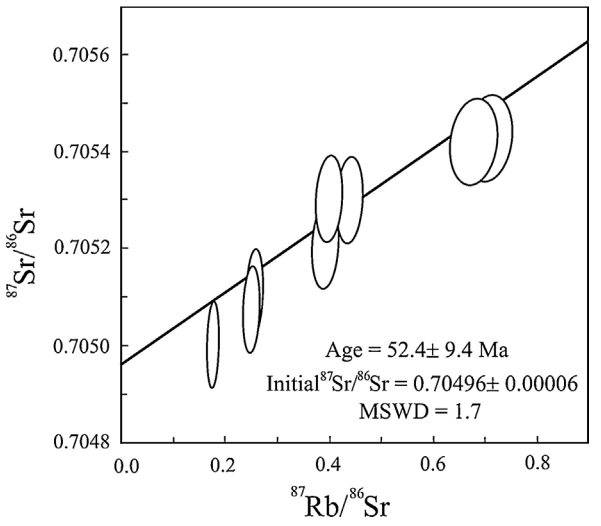

Fig. 5. Rb–Sr whole-rock isochron for 8 SG samples, shows an age of 52.4 ± 9.4 Ma. Data-point error ellipses are 2σ.

the characteristic of initial $^{87}Sr/^{86}Sr$ values less or more than 0.7060 for the I- and S-type granites, respectively.

4. Discussion

4.1. Magma source and fractional crystallization

As previously stated, the rocks of the Sirstan granitoids (SG) and the enclosing enclave have the characteristics of I-type granite. In the classification scheme, they have chemical signature of calc-alkaline magma in subduction zone environment. These rocks are part of magmatic arc as appeared in tectonic discrimination diagram of Pearce et al. (1984) (Fig. SM 6b), and are classified as orogenic granite as appeared in K/Rb vs. Rb/Sr diagram (Fig. SM 8a; Abdel-Rahman and El-Kibbi, 2001). The vast majority of SG rocks are plotted within the active continental margin (ACM) field, whereas the enclave sample shows oceanic arc affinity in the Ta/Yb–Th/Yb and Yb–Th/Ta diagrams (Fig. SM 8c, d: Gorton and Schandl, 2000). The enclave sample has Th/Ta ratio values reaching up to 27.4. In addition, the SG rock samples follow the assigned fractional crystallization trend (Fig. SM 8c).

The whole-rock geochemical characteristics, Sr–Nd isotopic data with positive ε_{Nd} (110 Ma) values (+0.1 to +2.7), and their clumped distribution within the mantle array in $^{87}Sr/^{86}Sr$–ε_{Nd} (110 Ma) diagram (Fig. SM 8b) indicate that the magma source for the SG rocks and the enclave lies in the mantle origin. Furthermore, the low values of Rb/Sr coupled with high Sm/Nd ratios (Table SM 1) let us infer that the parental magma of these rocks was generated by partial melting of a depleted mantle that underwent fractional crystallization when ascended into the continental crust. The geochemical aspects, including the relatively linear trend of the major and trace elements with SiO_2 (Fig. SM 4); the similarity of the REE patterns (Fig. 3) and the incompatible elements ratios (Fig. SM 8c) all support the role of the fractional crystallization in the evolution of the source magma of the SG rocks. Furthermore, the relationship of various trace elements and their ratios also support the effect of fractional crystallization in the evolution of the studied rocks. For example, the plots of Rb/Ba vs. Ti/Y ratios (Fig. SM 8e) show a random distribution and scattering of the plotted points. If the parental magma was contaminated or mixed with continental crustal components, then the trend of these rocks should be more or less linear and show increasing, i.e. these should be some sort of increase in the values of Rb/Ba and Ti/Y ratios. Also, on the plot giving the initial $^{143}Nd/^{144}Nd$ ratios vs. SiO_2 (Fig. SM 8f), the $^{143}Nd/^{144}Nd$ trend, which is almost a straight line, shows no considerable increase when SiO_2 increases. All these aspects in addition to the initial $^{87}Sr/^{86}Sr$ and ε_{Nd} (110 Ma) values indicate that neither contamination nor mixing with crustal components had any influence in the evolution of the magma, and that these rocks were most probably derived from the mantle and evolved through fractional crystallization processes.

Many propositions have been put to explain the genesis of the enclaves that occur with the granitoid rocks including enclaves of wall rock fragments magma mingling, restite and chilled margins (Barbarin, 1988; Barbarin and Didier, 1992; Chappell et al., 1987; Chen et al., 1990; Elburg, 1996; Kocak, 2006; Silva et al., 2000).

As previously noted, the enclave in the study area shows more or less similarities in their chemical compositions with the SG rocks in terms of the major and trace elements as well as the Sr–Nd isotopic ratios, which all indicate the cogenetic origin for both. However, the enclave sample is more mafic, containing higher contents of hornblende and biotite, with lesser alkalis; it is finer grained than the hosted SG rocks. It is peraluminous and shows oceanic arc affinity (Fig. SM 8c, d) and is relatively enriched in REE relative to the hosted granitoids. These lines of evidences more likely indicate that the enclave represents the earlier stage of evolution of the source magma than the SG rocks. In other words, the less evolved portion of the magma underwent the processes of the replenishment plus fractional crystallization (RFC) during the partial melting that had extracted the incompatible elements. The processes of RFC could be responsible for the observed trends of the REE and multi-elements (Fig. 3a, b) (e.g., Smith and Gray, 2011). However, more detailed studies are needed concerning the age of the enclaves in these rocks in order to provide reliable insights into their petrogenesis.

4.2. Middle Cretaceous igneous activity within the Zagros Belt

As previously discussed, the zircon U–Pb age of the SG rocks is 110 Ma, which indicates the existence of the igneous activity in SSZ during the Middle Cretaceous (i.e. Albian). The whole-rock Rb–Sr isochron for the SG rock samples yield rough estimated age of 52.4 ± 9.4 Ma, which is younger than the zircon U–Pb age. Although the estimated Rb–Sr isochron age (52.4 Ma) is not used here for magmatic geochronology, but probably gives reliable information about the timing of the tectonic and metamorphic events that occurred during the Paleogene period (i.e. Eocene) in

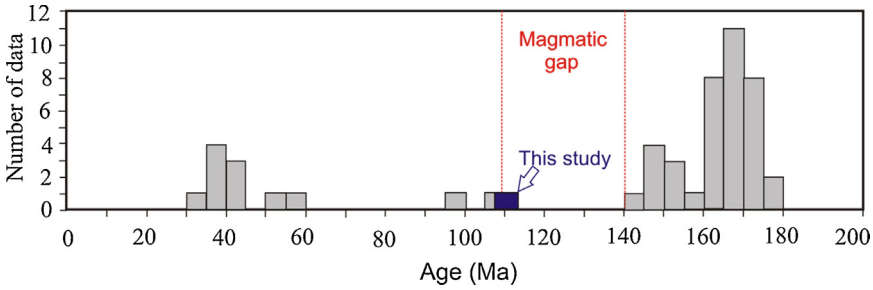

Fig. 6. Histogram of the age results of igneous rocks in the SSZ (after Chiu et al., 2013), showing the magmatic gap during the Cretaceous period.

northeastern Iraq and northwestern Iran within the Zagros Belt.

Chiu et al. (2013) reported a summary of the U–Pb zircon ages to constrain the magmatic evolution related to the Neo-Tethys subduction and the Zagros Orogeny during Mesozoic and Cenozoic times. They concluded that the highest magmatic activities in the SSZ had occurred during the Jurassic period (176–144 Ma). However, little is known about the magmatic activities during Early and Middle Cretaceous times (Fig. 6). Agard et al. (2011) concluded that the Middle to Late Cretaceous period (115–85 Ma) represents a specific time of perturbation of subduction marked by blueschist exhumation along the northern part of the Neo-Tethys subduction zone and the obduction processes in the southern part of the Neo-Tethys. Furthermore, this time is marked by rifting in the back-arc setting followed by closure during Late Cretaceous times with the development a supra subduction zone ophiolite (e.g., Agard et al., 2011; Ali, 2012; Ali et al., 2012; Shafaii Mogadam et al., 2009, 2014). Agard et al. (2005) suggested that the Middle to Late Cretaceous time recorded a change in the rates of convergence and speed of the Neo-Tethys subduction beneath SSZ. It is likely that the SG rocks were formed during the time of the perturbation of the subduction processes during the Middle Cretaceous time.

The geochemical and isotopic characteristics of the SG rocks indicate that these rocks came from partial melting of depleted mantle-derived materials above the subduction zone without significant contamination by continental crust. Furthermore, these features imply magmatic arc intrusion related to an active continental margin as the origin of the SG rocks. Based on our study, the zircon U–Pb age (110 Ma), which corresponds to the Middle Cretaceous adds new information about the magmatic activity that occurred in the Middle Cretaceous in the northern Arabian peninsula (northeastern Iraq) and northwestern Iran within the Zagros Belt.

5. Conclusions

The Sirstan granitoid body crops out in the northern Sanandaj–Sirjan Zone in northeastern Iraq. Zircon U–Pb dating shows that these rocks crystallized at 110 Ma. Chemical compositions and initial isotope ratios show that they are calc-alkaline granitoids that were generated in an active continental margin regime. Although the distribution of the Mesozoic granitoid bodies in the SSZ has shown that the main granitic bodies were crystallized during the period from 140 to 160 Ma, the SG granitoid with typical calc-alkaline magma in the active margin confirms the extending of granitoid bodies from the Middle Jurassic to the Middle Cretaceous in the northern SSZ. This clarifies a long period of Neo-Tethys subduction beneath the Iran. The whole-rock Rb–Sr isochron from fresh samples with 52 Ma probably suggests the heating of these rocks due to the collision of the Arabian and Iranian plates in the Cenozoic.

Acknowledgements

This research was financially supported by the Ministry of Higher Education and Scientific Research in Iraq and by JSPS KAKENHI grants No. 25303029 in Japan. I. Kadhim Abdulzahra would like to thank Nagoya University in Japan for supporting him as a Special Research Student during the period from November 2014 to October 2015 and the Iraq Geological Survey for support during the field trips. We also thank Ms. Masumi Nozaki (Nagoya University Museum) for SEM analysis, Prof. Makoto Takeuchi (Nagoya University) for zircon separation and Mr. Yoshikazu Kouchi (Toyama University, Japan) for advice about U–Pb age calculation.

We are grateful to Marc Chaussidon, Associate Editor of the journal, and the reviewers Philippe Boulvais and Ahmad Jahangiri for their constructive comments.

Appendix A. Supplementary data

Supplementary data associated with this article can be found, in the online version, at http://dx.doi.org/10.1016/j.crte.2017.02.004.

References

Abdel-Rahman, A.M., El-Kibbi, M.M., 2001. Anorogenic magmatism: chemical evolution of the Mount El-Sibai A-type complex (Egypt) and implications for the origin of within-plate felsic magmas. Geol. Mag. 138, 67–85.

Abdulzahra, I.K., Hadi, A., Asahara, Y., Azizi, H., Yamamoto, K., 2016. Zircon U–Pb ages and geochemistry of Devonian A-type granites in the Iraqi Zagros suture zone (Damamna area): new evidence for magmatic activity related to the Hercynian Orogeny. Lithos 264, 360–374.

Agard, P., Omrani, J., Jolivet, L., Whitechurch, H., Vrielynck, B., Spakman, W., Monie, P., Meyer, B., Wortel, R., 2011. Zagros orogeny: a subduction-dominated process. Geol. Mag. 148, 692–725.

Agard, P., Omrani, J., Jolivet, L., Mouthereau, F., 2005. Convergence history across Zagros (Iran): constraints from collisional and earlier deformation. Geol. Rundsch. 94, 401–419.

Ahmadi Khalaji, A., Esmaeily, D., Valizadeh, M.V., Rahimpour-Bonab, H., 2007. Petrology and geochemistry of the granitoid complex of Boroujerd, Sanandaj–Sirjan Zone, Western Iran. J. Asian Earth Sci. 29, 859–877.
Alavi, M., 1980. Tectonostratigraphic evolution of Zagrosides of Iran. Geology 8, 144–149.
Alavi, M., 1994. Tectonic of the Zagros orogenic belt of Iran: new data and interpretations. Tectonophysics 229, 211–238.
Al-Hafdh, N.M., Qasim, S.A., 1992. Petrochemistry and geotectonic setting of the Shalair granite, NE Iraq. J. Afr. Earth Sci. 14, 429–441.
Ali, S.A., 2012. Geochemistry and geochronology of Tethyan-arc related igneous rocks, NE Iraq. University of Wollongong, Ph. D thesis, (324p).
Ali, S.A., Buckman, S., Aswad, K.J., Jones, B.G., Ismail, S.A., Nutman, A.P., 2012. Recognition of Late Cretaceous Hasanbag ophiolite-arc rocks in the Kurdistan Region of the Iraqi Zagros suture zone: a missing link in the paleogeography of the closing Neotethys Ocean. Lithosphere 4, 395–410.
Ali, S.A., Ismail, S.A., Nutman, A.P., Bennett, V.C., Jones, B.G., Buckman, S., 2016. The intra-oceanic Cretaceous (~ 108 Ma) Kata-Rach arc fragment in the Kurdistan segment of Iraqi Zagros suture zone: implications for Neotethys evolution rocks closure. Lithos 260, 154–163.
Alirezaei, S., Hassanzadeh, J., 2012. Geochemistry and zircon geochronology of the Permian A-type Hasanrobat granite. Sanandaj-Sirjan belt: a new record of the Gondwana break-up in Iran. Lithos 151, 122–134.
Allègre, C.J., 2008. Isotope Geology. Univ. Press, Cambridge.
Al-Rubaie, S.H., 1976. Granitic and trondhjemitic intrusions in the Shlair Valley. University of Baghdad, NE Iraq133 (M. Sci. thesis).
Al-Shible, T.A., Kettaneh, Y.A., 1972. Reconnaissance radiometric and geology in NE Penjwin (Shalair Valley). Iraqi Atomic Energy Commission Report. (36 p).
Armstrong, R.L., Taubeneck, W.H., Hales, P.O., 1977. Rb-Sr and K-Ar geochronometry of Mesozoic granitic rocks and their Sr isotopic composition, Oregon, Washington, and Idaho. Geol. Soc. Am. Bull. 88, 397–411.
Asmerom, Y., Damon, P., Shafiqullah, M., Dickinson, W.R., Zartman, R.E., 1991. Resetting of Rb–Sr ages of volcanic rocks by low-grade burial metamorphism. Chem. Geol. 87, 167–173 (Isotope Geoscience Section).
Azizi, H., Jahanjiri, A., 2008. Cretaceous subduction–related volcanism in the northern Sanadaj-Sirjan Zone. Iran. J. Geodyn. 45, 178–190.
Azizi, H., Moinevaziri, H., 2009. Review of the tectonic setting of Cretaceous to Quaternary volcanism in the northwestern Iran. J. Geodyn. 47, 167–179.
Azizi, H., Asahara, Y., Mehrabi, B., Chung, S.L., 2011. Geochronological and geochemical constraints on the petrogenesis of high-K granite from the Suffi abad area, Sanandaj–Sirjan zone, NW Iran. Chem. Erde 71, 363–376.
Azizi, H., Beiranvand, M.Z., Asahara, Y., 2015. Zircon U–Pb ages and petrogenesis of a tonalite-trondhjenite-granodiorite (TTG) complex in the northern Sanadaj-Sirjan zone, Northwest Iran; Evidence for Late Jurassic arc continent-collision. Lithos 216-217, 178–195.
Baharifar, A., Moinevaziri, H., Bellon, H., Piqué, A., 2004. The crystalline complexes of Hamadan (Sanandaj–Sirjan zone, western Iran): metasedimentary Mesozoic sequences affected by Late Cretaceous tectono-metamorphic and plutonic events. C. R. Geoscience 336, 1443–1452.
Barbarin, B., Didier, J., 1992. Genesis and evolution of mafic microgranular enclaves through various types of interaction between coexisting felsic and mafic magmas. Trans. R. Soc. Edinb. Earth Sci 83, 145–153.
Barbarin, B., 1988. Field evidence for successive mixing and mingling between the Piolard Diorite and the Saint-Julien-la-Vetre monzogranite (Nord-Forez, Massif Central France). Can. J. Earth Sci. 25, 49–59.
Bea, F., Mazhari, A., Montero, P., Amini, S., Ghalamghash, J., 2011. Zircon dating, Sr and Nd isotopes, and element geochemistry of the Khalifan pluton, NW Iran: evidence for Variscan magmatism in a supposedly Cimmerian superterrane. J. Asian Earth Sci. 40, 172–179.
Berberian, F., Berberian, M., 1981. Tectono-plutonic episodes in Iran. In: Gupta, H.K., Delany, F.M. (Eds.), Zagros-Hindu Kush-Himalaya Geodynamic Evolution, 3, American Geophysical Union, Geodynamics Series, Washington, DC, pp. 5–32.
Berberian, M., King, C.C.P., 1981. Toward a paleogeography and tectonic evolution of Iran. Can. J. Earth Sci. 18, 210–265.
Buday, T., Jassim, S.Z., 1987. The regional geology of Iraq. Tectonism, magmatism and metamorphism, 2. Publication of GEOSURV, Baghdad, Iraq (352p).
Chappell, B.W., White, A.R.J., 1974. Two contrasting granite types. Pacific Geology 8, 173–174.
Chappell, B.W., White, A.J.R., 1992. I- and S- type granites in the Lachlan Fold Belt. Trans. R. Soc. Edinb. Earth Sci. 83, 1–26.
Chappell, B.W., White, A.J.R., Wyborn, D., 1987. The importance of residual source material (restite) in granite petrogenesis. J. Petrol. 28, 1111–1138.
Chen, R.X., Zheng, Y.F., Zhao, Z.F., Tang, J., Wu, F.Y., Liu, X.M., 2007. Zircon U–Pb ages and Hf isotopes in ultrahigh-pressure metamorphic rocks from the Chinese Continental Scientific Drilling project. J. Metamorph. Geol. 25, 873–894.
Chen, Y.D., Price, R.C., White, A.J.R., Chappell, B.W., 1990. Mafic inclusions from the Glenbog and Blue Gum Granite Suites, southeastern Australia. J. Geophys. Res. 95, 17757–17785.
Chiu, H., -Y, Chung, S., Zarrinkoub, M.H., Mohammadi, S.S., Khatib, M.M., Iizuka, Y., 2013. Zircon U–Pb age constraints from Iran on the magmatic evolution related to Neotethyan subduction and Zagros orogeny. Lithos 162–163, 70–87.
De Villiers, P.R., 1957. The geology of the Shaliar Valley, Report No. 270/52. GEOSURV, Baghdad, Iraq.
Esna-Ashari, A., Tiepolo, M., Valizadeh, M.-V., Hassanzadeh, J., Sepahi, A.-A., 2012. Geochemistry and zircon U–Pb geochronology of Aligoodarz granitoid complex, Sanandaj–Sirjan Zone, Iran. J. Asian Earth Sci. 43, 11–22.
Elburg, M.A., 1996. Evidence of isotopic equilibration between microgranitoid enclaves and host granodiorite, Warburton Granodiorite, Lachlan Fold Belt, Australia. Lithos 38, 1–22.
Evans, J.A., 1995. Mineral and isotope features related to resetting of Rb–Sr whole-rock isotope systems during low grade metamorphism. Geol. Soc. Am. Bull., Spec. Pubi. 296, 157–169.
Fazlnia, A., Schenk, V., van der Straaten, F., Mirmohammadi, M., 2009. Petrology, geochemistry, and geochronology of trondhjemites from the Qori Complex, Neyriz, Iran. Lithos 112, 413–433.
Ghasemi, A., Talbot, C.J., 2006. A new tectonic scenario for the Sanandaj–Sirjan Zone (Iran). J. Asian Earth Sci. 26, 683–693.
Gorton, M.P., Schandl, E.S., 2000. From continents to island arcs: A geochemical index of tectonic setting for arc-related and within-plate felsic to intermediate volcanic rocks. Can. Mineral. 38, 1065–1073.
Hartmann, L.A., Santos, J.O.S., 2004. Predominance of high Th/U, magmatic zircon in Brazilian Shield sandstones. Geology 32, 73–76.
Hassanzadeh, J., Wernicke, B.P., 2016. The Neotethyan Sanandaj–Sirjan zone of Iran as an archetype for passive margin-arc transitions. Tectonics 35 (3), 586–621.
Hassanzadeh, J., Stockli, D.F., Horton, B.K., Axen, G.J., Stockli, L.D., Grove, M., Schmitt, A.K., Walker, J.D., 2008. U–Pb zircon geochronology of late Neoproterozoic–Early Cambrian granitoids in Iran: implications for paleogeography, magmatism and exhumation history of Iranian basement. Tectonophysics 451 (1–4), 71–96.
Hoskin, P.W.O., Schaltegger, U., 2003. The composition of zircon and igneous and metamorphic petrogenesis. Rev. Mineral. Geochem. 53, 27–62.
Irvine, T.N., Baragar, W.R.A., 1971. A guide to the chemical classification of the common volcanic rocks. Can. J. Earth Sci. 8, 523–548.
Jassim, S.Z., Goff, J.C., 2006. Geology of Iraq. Dolin, Paragues and Moravian Museum Brno (341p).
Kazmin, V.G., 1991. Collision and rifting in the Tethys Ocean: geodynamic implications. Tectonophysics 196, 371–384.
Kocak, K., 2006. Hybridization of mafic microgranular enclaves: mineral and whole-rock chemistry evidence from the Karamadazi Granitoid, Central Turkey. Int. J. Earth Sci. 95, 587–607.
Ludwig, K.R., 2012. Isoplot, a geochronological toolkit for Microsoft Excel. Berkeley Geochronology Center. Spec. Publ. 5, 75.
Mahmoudi, S., Corfu, F., Masoudi, F., Mehrabi, B., Mohajjel, M., 2011. U–Pb dating and emplacement history of granitoid plutons in the northern Sanandaj–Sirjan zone, Iran. J. Asian Earth Sci. 41, 238–249.
Masoudi, F., Yardley, B.W.D., Cliff, R.A., 2002. Rb–Sr geochronology of pegmatites, plutonic rocks and a hornfels in the region southwest of Arak. Iran. J. Sci., I. R. Iran 13, 249–254.
Mazhari, S.A., Bea, F., Amini, S., Ghalamghash, J., Molina, J.F., Montero, P., Scarrow, J.H., Williams, I.S., 2009. The Eocene bimodal Piranshahr massif of the Sanandaj- Sirjan Zone, West Iran: a marker of the end of collision in the Zagros orogen. J. Geol. Soc., London 166, 53–69.
Mazhari, S.A., Amini, S., Ghalamghash, J., Bea, F., 2011. Petrogenesis of granitic unit of Naqadeh complex, Sanandaj–Sirjan Zone, NW Iran. Arab. J. Geosci. 4, 59–67.
Middlemost, E.A.K., 1985. Magmas and Magmatic Rocks. Longman, London (266 p.).
Mohajjel, M., Fergusson, C.L., Sahandi, M.R., 2003. Cretaceous–Tertiary convergence and continental collision, Sanandaj–Sirjan Zone, western Iran. J. Asian Earth Sci. 21, 397–412.
Omrani, J., Agard, P., Whitechurch, H., Mathieu Benoit, M., Prouteau, G., Jolivet, L., 2008. Arc-magmatism and subduction history beneath the Zagros Mountains, Iran: A new report of adakites and geodynamic consequences. Lithos 106, 380–398.

Pearce, J.A., Harris, N.B.W., Tindle, A.G., 1984. Trace-element discrimination diagrams for the tectonic interpretation of granitic-rocks. J. Petrol. 25, 956–983.
Pitcher, W.S., 1979. The nature, ascent and emplacement of granitic magmas. J. Geol. Soc., London 136, 627–662.
Rubatto, D., 2002. Zircon trace element geochemistry: partitioning with garnet and the link between U–Pb ages and metamorphism. Chem. Geol. 184, 123–138.
Sengor, A.M.C., 1990. A new model for the late Paleozoic-Mesozoic tectonic evolution of Iran and implications for Oman. Geol. Soc., London, Spec. Publ. 49, 797–831.
Sepahi, A.-A., Shahbzi, H., Siebel, W., Ranin, A., 2014. Geochronology of plutonic rocks from the Sanandaj–Sirjan zone. Iran and new zircon and titanite U–Th–Pb ages for granitoids from the Marivan pluton. Geochronometria 41, 207–215.
Shafaii Mogadam, H.S., Khedr, M.Z., Chiaradia, M., Stern, R.J., Bakhshizad, F., Arai, S., Ottley, C.J., Tamura, A., 2014. Supra-subduction zone magmatism of the Neyriz ophiolite. Iran: constraints from geochemistry and Sr-Nd-Pb isotopes. Int. Geol. Rev. 56, 1395–1412.
Shafaii Mogadam, H.S., Li, X.H., Ling, X.X., Stern, R.J., Santos, J.F., Meinhold, G., Ghorbani, G., Shahabi, S., 2015. Petrogenesis and tectonic implications of Late Carboniferous A-type granites and gabbronorites in NW Iran: geochronological and geochemical constraints. Lithos 212–215 (266–279).
Shafaii Mogadam, H.S., Whitechurch, H., Monsef, I., Rahgoshay, M., 2009. Significance of Nain-Baft ophiolitic belt (Iran): Short-lived, transtensional Cretaceous back-arc oceanic basins over the Tethyan subduction zone. C. R. Geoscience 341, 1016–1028.
Shahbazi, H., Siebel, W., Pourmoafee, M., Ghorbani, M., Sepahi, A.A., Shang, C.K., Vousoughi Abedini, M., 2010. Geochemistry and U–Pb zircon geochronology of the Alvand plutonic complex in Sanandaj–Sirjan zone (Iran): new evidence for Jurassic magmatism. J. Asian Earth Sci. 39, 668–683.
Shakerardakani, F., Neubauer, F., Masoudi, F., Mehrabi, B., Liu, X., Dong, Y., Mohajjel, M., Monfaredi, B., Friedl, G., 2015. Panafrican basement and Mesozoic gabbro in the Zagros orogenic belt in the Dorud–Azna region (NW Iran): laser-ablation ICP–MS zircon ages and geochemistry. Tectonophysics 647–648 (146-171).
Shand, S.J., 1943. 2nd edn. The Eruptive Rocks, 2nd edn, John Wiley, New York, pp. 444.
Sharland, P.R., Archer, R., Casey, D.M., Davies, R.B., Hall, S.H., Heward, A.P., Horbury, A.D., Simmons, M.D., 2001. Arabian plate sequence stratigraphy, 2. GeoArabia, Spec. Publ., Bahrain (371 p. and 3 enclosures).
Silva, M.M.V.G., Neiva, A.M.R., Whitehouse, M.J., 2000. Geochemistry of enclaves and host granites from the Nelas area, central Portugal. Lithos 50, 153–170.
Smirnov, V.A., Nelidov, V.P., 1962. Report on 1:2,0000 prospecting correlation of the Sylaimaniya-Choarta and Penjwin area carried out in 1961. GEOSURV, Baghdad, Iraq46 (Report No. 290).
Smith, R.K., Gray, W., 2011. Geochemistry and petrogenesis of Mesoproterozoic (~ 1.1 Ga) magmatic enclaves in granites of the eastern Llano Uplift, central Texas, USA. Lithos 125, 463–481.
Sun, S.S., McDonough, W.F., 1989. Chemical and isotopic systematic of oceanic basalts: implication for mantle composition and processes. In: Sunders, A.D., Norry, M.J. (Eds.), Magmatic in Oceanic Basins, 42, Geol. Soc. London, Spec. Publ., pp. 313–345.
Vergès, J., Saura, E., Casciello, E., Fernàndez, M., Villaseñor, A., Jiménez-Munt, I., García-Castellanos, D., 2011. Crustal-scale cross-sections across the NW Zagros belt: implications for the Arabian margin reconstruction. Geol. Mag. 148, 739–761.
Whalen, J.B., Currie, K.L., Chappell, B.W., 1987. A-Type granites: geochemical characteristics, discrimination and petrogenesis. Contrib. Mineral. Petrol. 95, 407–419.

Further reading

Azizi, H., Asahara, Y., 2013. Juvenile granite in the Sanandaj–Sirjan zone NW Iran: Late Jurassic-Early Cretaceous arc-continent collision. Int. Geol. Rev. 55, 1523–1540.
DePaolo, D.J., Wasserburg, G.J., 1976. Nd isotopic variations and petrogenetic models. Geophys. Res. Lett. 3, 249–252.
Goolaerts, A., Mattielli, N., De Jong, J., Weis, D., Scoates, J.S., 2004. Hf and Lu reference values for the zircon standard 9,1500 by MC-ICP-MS. Chem. Geol. 206, 1–9.
Kouchi, Y., Orihashi, Y., Obara, H., Fujimoto, T., Haruta, Y., Yamamoto, K., 2015. Zircon U–Pb dating by 213 nm Nd: YAG laser ablation inductively coupled plasma mass spectrometry: optimization of the analytical condition to use NIST SRM 610 for Pb/U fractionation correction. Chikyukagaku (Geochemistry) 49, 19–35 (in Japanese with English abstract).
Orihashi, Y., Nakai, S. Hirata, T., 2008. U–Pb Age determination for seven standard zircons using inductively coupled plasma–mass spectrometry coupled with frequency quintupled Nd-YAG (λ = 213 nm) laser ablation system: comparison with LA-ICP-MS zircon analyses with a NIST glass reference material. Resour. Geol. 58, 101–123.
Stacey, J.T., Kramers, J.D., 1975. Approximation of terrestrial lead isotope evolution by a two-stage model. Earth Planet. Sci. Lett. 26, 207–221.
Tanaka, T., Togashi, S., Kamioka, H., Amakawa, H., Kagami, H., Hamamoto, T., Yuhara, M., et al., 2000. JNdi-1: a neodymium isotopic reference in consistency with LaJolla neodymium. Chem. Geol. 168, 279–281.